SOGI-based Flexible Grid Connection of PV Power Three Phase Converters under Non-ideal Grid Conditions

Rabeh Abbassi
College of Engineering, University of Hail, Hail, Kingdom of Saudi Arabia
University of Tunis, ENSIT, LaTICE Laboratory, Tunisia
Higher Institute of Applied Sciences and Technology of Kasserine, University of Kairouan, Tunisia
r_abbassi@yahoo.fr

Abstract—**This paper proposes a control strategy of improving the power quality of the energy exchanged between a photovoltaic generator (PVG) and an unbalanced grid. A voltage source inverter (VSI) allowing the control of the zero-sequence during unbalanced regimes is proposed. A Second-Order Generalized Integrators-Based Approach (SOGI-BA), which suitably fits with the network's imbalances while ensuring the perfect isolation of the PVG from the adverse effects of the imbalance, is investigated. The investigation will focus mainly on three control objectives: the generation of a balanced current system, the active and reactive power's dependent control, and the elimination of the second frequency DC bus voltage fluctuations. The performance of this new approach is approved by various tests via MATLAB environment simulations.**

Keywords-power quality; photovoltaic generator; voltage source inverter; active and reactive power dynamic control; voltage ride-through; ancillary services; symmetrical components; SOGI integrators

I. INTRODUCTION

Electronic power converters are a technology that allows efficient and flexible interconnection of different types of generators to the utility grid [1-3]. With the growing trend to increase the integration rate of distributed generation based on renewable energy systems (RES), it is required to pay a particular attention to converters interfacing with the grid [4-5]. This requirement is a result of their important role as “synchronous converters” in future power systems. This is analogous to the critical role that the synchronous machines play in centralized power systems [6]. In addition, the role of the filter, usually dominated by inductors, remains crucial especially during the transitional operation phases. Moreover, a further complication that derives from the management of the fluctuating power produced by the distributed generation systems, leads to the use of multiple voltage levels and thus more complex structures of converters [7]. Also, challenges and opportunities for the design and control of the grid side converter (GSC) are strongly related to the availability of new powerful and intelligent computing devices [8-10]. These devices must be controlled to obey the need to operate with the lowest possible switching frequency in order to control the highest power level.

Various control schemes for balancing the output voltages of the grid-side converter (GSC) have been published [11-17]. The majority of them relies on vector (dq) control. A current and voltage dual-loop control method relying on instantaneous active and reactive power theory is suggested for the GSC in [3]. Although this method shows excellent performance under balanced grid states, it is unable to convert AC quantities to DC quantities allowing PI controllers to process them quickly while ensuring zero error in steady-state [4]. However, under faulty grid conditions, the apperance of the negative sequence decreases the control accuracy. To resolve these drowbaks, an improved approach using a 4-leg inverter is suggested in [5] to allow a relatively low degree of imbalance. Five reference current generation techniques have been developped in [18-19] to generate sinusoidal currents of the symmetrical sequences. In the same context, a simplified repetitive predictor-based grid-voltage feed forward approach has been designed for grid-tied high-power VSI [16]. A phase locked loop-free sliding-mode-based power control for grid-tied VSIs under unbalanced grid conditions has been proposed in [21]. In addition to the emphasis on design and control of converters connected to the network, other basic and advanced topics related to synchronization with the network and control of PV systems under grid defects have been analyzed in [22-24].

To address the above issues, the present paper proposes an oriented control contribution to implement new concepts to remedy the interaction of the symmetrical components and thus manage the oscillations of the active and reactive powers. This contribution will aim achieving the safety of the operation and the continuity of service of the photovoltaic generator (PVG) connected to the distribution network. In order to ensure a coordinated control of the active and reactive powers for a better integration of a PVG into an unbalanced electrical grid, new control algorithms for the GSC during grid imbalances are proposed below. After presenting the PV generator modeling and control, the main objectives of this work are:

Corresponding author: Rabeh Abbassi

- To introduce symmetrical sequence generation using fortescue theory and its drawbaks.
- To develop and implement in MATLAB the proposed SOGI-BA control algorithms for the GSC with LCL Filter.
- To present and discuss the results of time domain simulations under various symmetrical and asymmetrical conditions.
- To outline the conclusions and suggest future work.

II. PV GENERATOR MODELING AND CONTROL

Accuracy is the most important factor to take into consideration when selecting an appropriate simulation model. The system configuration adopted in this work is the intermediate DC bus one depicted in Figure 1.

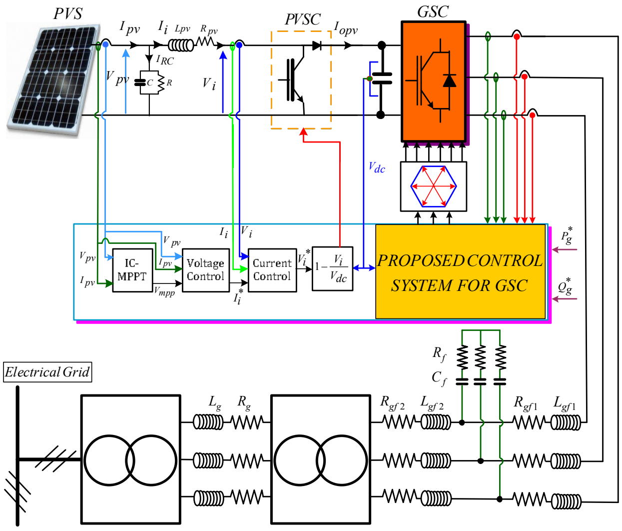

Fig. 1. ON-grid PV system used in simulations

This decision is dictated by the importance of both the DC-DC converter responsible for the maximum power point tracking and the DC-AC inverter to prevent the total and immediate stoppage of the energy production in case a problem occurs upstream of this converter [3]. A detailed modeling of the chosen model has been presented in [5].

III. INTRODUCTION TO SYMMETRICAL SEQUENCES GENERATION

A. Using Fortescue Theory

Traditionally, the analysis of three-phase systems has been carried out thanks to the symmetrical components making it possible to easily extract the characteristic information of such systems. The transformation of the space vector is derived from that of the symmetric components. The Fortescue transformation, applicable to sinusoidal function phasors, allows the analysis of asymmetrical three-phase systems under sinusoidal conditions. The application of this transform to temporal quantities is given by (1), (2) and (3) leading to positive, negative and zero sequences, respectively [5]:

$$\begin{bmatrix} \underline{v}_a^P \\ \underline{v}_b^P \\ \underline{v}_c^P \end{bmatrix} = \begin{bmatrix} V_P \cdot e^{(j\cdot\omega_g\cdot t+\varphi_P)} \\ V_P \cdot e^{(j\cdot\omega_g\cdot t-\frac{2\cdot\pi}{3}+\varphi_P)} \\ V_P \cdot e^{(j\cdot\omega_g\cdot t+\frac{2\cdot\pi}{3}+\varphi_P)} \end{bmatrix} = [F_P]\cdot\begin{bmatrix} \underline{v}_a \\ \underline{v}_b \\ \underline{v}_c \end{bmatrix} = \frac{1}{3}\cdot\begin{bmatrix} 1 & a & a^2 \\ a^2 & 1 & a \\ a & a^2 & 1 \end{bmatrix}\cdot\begin{bmatrix} \underline{v}_a \\ \underline{v}_b \\ \underline{v}_c \end{bmatrix} \quad (1)$$

$$\begin{bmatrix} \underline{v}_a^N \\ \underline{v}_b^N \\ \underline{v}_c^N \end{bmatrix} = \begin{bmatrix} V_N \cdot e^{(j\cdot\omega_g\cdot t+\varphi_N)} \\ V_N \cdot e^{(j\cdot\omega_g\cdot t+\frac{2\cdot\pi}{3}+\varphi_N)} \\ V_N \cdot e^{(j\cdot\omega_g\cdot t-\frac{2\cdot\pi}{3}+\varphi_N)} \end{bmatrix} = [F_N]\cdot\begin{bmatrix} \underline{v}_a \\ \underline{v}_b \\ \underline{v}_c \end{bmatrix} = \frac{1}{3}\cdot\begin{bmatrix} 1 & a^2 & a \\ a & 1 & a^2 \\ a^2 & a & 1 \end{bmatrix}\cdot\begin{bmatrix} \underline{v}_a \\ \underline{v}_b \\ \underline{v}_c \end{bmatrix} \quad (2)$$

$$\begin{bmatrix} \underline{v}_a^Z \\ \underline{v}_b^Z \\ \underline{v}_c^Z \end{bmatrix} = \begin{bmatrix} V_Z \cdot e^{(j\cdot\omega_g\cdot t+\varphi_Z)} \\ V_Z \cdot e^{(j\cdot\omega_g\cdot t+\varphi_Z)} \\ V_Z \cdot e^{(j\cdot\omega_g\cdot t+\varphi_Z)} \end{bmatrix} = [F_Z]\cdot\begin{bmatrix} \underline{v}_a \\ \underline{v}_b \\ \underline{v}_c \end{bmatrix} = \frac{1}{3}\cdot\begin{bmatrix} 1 & 1 & 1 \\ 1 & 1 & 1 \\ 1 & 1 & 1 \end{bmatrix}\cdot\begin{bmatrix} \underline{v}_a \\ \underline{v}_b \\ \underline{v}_c \end{bmatrix} \quad (3)$$

where : $a = e^{j\cdot\frac{2.\pi}{3}}$.

B. Positive Sequence Calculation on αβ Reference Frame

The Clarke transformation can be applied to calculate the components of the *abc* voltage vector in the *αβ* reference frame:

$$\begin{bmatrix} v_\alpha \\ v_\beta \end{bmatrix} = [T_{\alpha\beta}]\cdot\begin{bmatrix} v_a \\ v_b \\ v_c \end{bmatrix} = \frac{2}{3}\cdot\begin{bmatrix} 1 & -\frac{1}{2} & -\frac{1}{2} \\ 0 & \frac{\sqrt{3}}{2} & -\frac{\sqrt{3}}{2} \end{bmatrix}\cdot\begin{bmatrix} v_a \\ v_b \\ v_c \end{bmatrix} \quad (4)$$

In the same reference frame, the instantaneous positive sequence voltage can be expressed by (5):

$$\begin{aligned} \begin{bmatrix} v_\alpha^P \\ v_\beta^P \end{bmatrix} &= [T_{\alpha\beta}]\cdot\begin{bmatrix} v_a^P \\ v_b^P \\ v_c^P \end{bmatrix} = [T_{\alpha\beta}]\cdot[F_P]\cdot\begin{bmatrix} v_a \\ v_b \\ v_c \end{bmatrix} \\ &= [T_{\alpha\beta}]\cdot[F_P]\cdot[T_{\alpha\beta}]^{-1}\cdot\begin{bmatrix} v_\alpha \\ v_\beta \end{bmatrix} \quad (5) \\ &= \frac{1}{2}\begin{bmatrix} 1 & -e^{-j\frac{\pi}{2}} \\ -e^{-j\frac{\pi}{2}} & 1 \end{bmatrix}\cdot\begin{bmatrix} v_\alpha \\ v_\beta \end{bmatrix} = \frac{1}{2}\begin{bmatrix} 1 & -q \\ -q & 1 \end{bmatrix}\cdot\begin{bmatrix} v_\alpha \\ v_\beta \end{bmatrix} \end{aligned}$$

In time-domain, *q* is defined as a phase-shift operator [25]. It allows the generation of the quadrature-phase signal (90-degrees lag) of the original in-phase signal of *αβ* voltage vector. A disadvantage of Fortescue components is that the transformation matrix is complex, which poses serious difficulties. For these reasons and others, new techniques such as SOGI have been proposed for the synthesis of symmetric sequences.

IV. SYSTEM CONFIGURATION OF SOGI-BASED CONTROL FOR GSC WITH LCL FILTER

A. SOGI for Quadrature Signal Generation (QSG)

To generate 90 degrees phase shifted signals of the components v_α and v_β, various techniques are conceivable.

Given the inadequacy of these techniques, in this work we have resorted to the use of a generalized second-order integrator-based PLL (SOGI-PLL) [12-13] whose base is illustrated in Figure 2. The transfer function is as follows:

$$\begin{aligned} D(s) &= \frac{v'}{v}(s) = \frac{k\omega' s}{s^2 + k\omega' s + \omega'^2} \\ Q(s) &= \frac{qv'}{v}(s) = \frac{k\omega'^2}{s^2 + k\omega' s + \omega'^2} \end{aligned} \qquad (6)$$

k and *ω'* are the damping factor and set resonance frequency of the SOGI-QSG, respectively.

For the sinusoidal grid voltage with frequency *ω*, the *dq* SOGI-QSG outputs of the phasor *v* are expressed by (7) and (8), respectively:

$$\mathrm{v}' = \mathrm{D}.\mathrm{v} = |\mathrm{D}|.e^{j\underline{|\mathrm{D}}}.\mathrm{v}$$
$$\begin{cases} |\mathrm{D}| = m_{\mathrm{D}} = \dfrac{k\omega\omega'}{\sqrt{(k\omega\omega')^2 + (\omega^2 - \omega'^2)^2}} \\ \underline{|\mathrm{D}} = \theta_{\mathrm{D}} = \tan^{-1}\left(\dfrac{\omega'^2 - \omega^2}{k\omega\omega'}\right) \end{cases} \qquad (7)$$

$$\mathrm{q.v}' = \mathrm{Q}.\mathrm{v} = |\mathrm{Q}|.e^{j\underline{|\mathrm{Q}}}.\mathrm{v}$$
$$\begin{cases} |\mathrm{Q}| = m_{\mathrm{Q}} = \dfrac{\omega'}{\omega}.m_{\mathrm{D}} \\ \underline{|\mathrm{D}} = \theta_{\mathrm{Q}} = \theta_{\mathrm{Q}} - \dfrac{\pi}{2} \end{cases} \qquad (8)$$

Based on the previous mathematical foundations, the shematic of double SOGI-QSG-based symmetrical sequences generation (DSOGI-QSG) is depicted in Figure 3 [25].

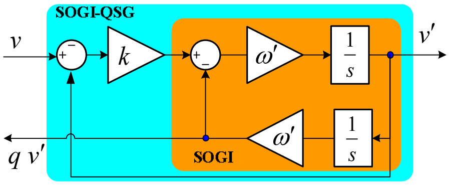

Fig. 2. Equivalent schematic of the SOGI-QSG

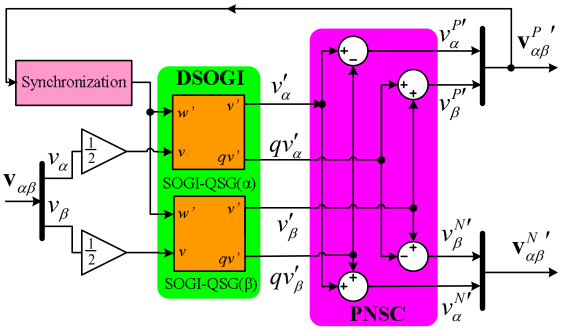

Fig. 3. DSOGI-QSG based symmetrical sequences generation

After having generated the symmetrical sequences' components referring to the stationary reference frame *αβ*, the following section focuses on the implementation of the proposed control approach in case of the connection of the GPV to an unbalanced grid via the GSC and an LCL filter.

B. *LCL filtering Model*

As shown in Figure 1, the passive damping at the LCL filter is ensured by the resistors in series with the capacitor [19]. If no damping resistors are integrated, the transfer function is:

$$v_{F,d}(s) = \frac{1}{L_{gf1}C_f L_{gf2}s^3 + (L_{gf1} + L_{gf2})s} \qquad (9)$$

Otherwise, in the presence of filter damping resistors, such a function is rewritten:

$$v_{F,d}(s) = \frac{C_f R_f s + 1}{L_{gf1}C_f L_{gf2}s^3 + C_f(L_{gf1}L_{gf2})R_f s^2 + (L_{gf1} + L_{gf2})s} \qquad (10)$$

The main contribution of the resistors R_f is to attenuate the peak of the filter transfer function when only the inductive and capacitive elements are present.

C. *Proportional Resonant Current Controller for the Inner Loop Control of GSC*

For the GSC inverter, one of the key objectives is the accuracy of the inner loop control of the converter. Knowing that various types of controllers can be introduced to ensure this task, the proportional resonant (PR) current controller is used in this paper thanks to the simplicity of its implementation and its solid performance. However, it should be noted that for reasons of stability, which require the implementation of a damped or bandpass structure, the transfer function is expressed by:

$$G_{PR}(s) = K_p + K_r \frac{s}{s^2 + 2\omega_c s + \omega_0^2} \qquad (11)$$

D. *Current Reference Generation*

Under unbalanced conditions, the simplest strategy for power control is to keep the injected currents into the grid sinusoidal and balanced. This is the subject of the Balanced Positive Sequence Control (BPSC) [25]. The main scheme of the proposed control approach is depicted by the schematic in Figure 4. If the quality of such currents is crucial, only the components of the positive sequence of the grid voltages is used to calculate the grid currents references as follows:

$$i^{P*} = \frac{P_g^*}{\left\|v^P\right\|^2} \cdot v^P = g^P \cdot v^P \qquad (12)$$

The reference current vector i^{P*} is perfectly sinusoidal and balanced. Under unbalanced conditions, the instantaneous active power delivered at the point of common coupling (PCC) is different from its reference P_g^* due to the interaction between the positive sequence of the injected current i^{P*} and the negative sequence of the grid voltage v^{N*}. Indeed:

$$P_g^* = v\ .i^{P*} = \overbrace{v^P .i^{P*}}^{P_g^*} + \overbrace{v^N .i^{P*}}^{\tilde{p}_{2\omega}} \qquad (13)$$

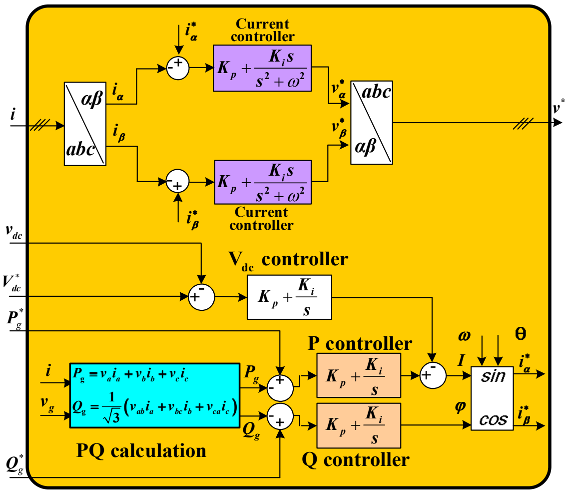

Fig. 4. Schematic of the proposed SOGI-BA

Here, $\tilde{p}_{2\omega}$ is the power fluctuating at the second harmonic frequency. If the reference of the reactive power Q_g^* is set to zero, its instantaneous value can be calculated as:

$$Q_g = \left\| v\ .i^{P*} \right\| = \overbrace{v^P .i^{P*}}^{0} + \overbrace{v^N .i^{P*}}^{\tilde{q}_{2\omega}} \qquad (14)$$

where $\tilde{q}_{2\omega}$ is the amount of reactive power oscillating at twice the fundamental grid frequency. In order to provide a smooth tracking capability and achieve zero error during the steady state condition, PR current controllers are applied for the inner current control loop of the GSC inverter.

V. SIMULATION RESULTS AND DISCUSSIONS

This section focuses on the MATLAB simulation results of the proposed algorithms. A detailed comparative study was carried out to highlight the performance of the DSOGI-BA. The structure of the implemented simulation model consists of a grid-tied PV system, as presented in Figure 1, where two power electronics converters ensure the interfacing with the grid. The first one is the MPPT-controlled boost DC-DC converter. The second is the grid-side converter delivering 15kW to the grid. The simulated fault consists of a three-phase voltage drop affecting the three phases of the network with respective decreases of 75%, 50% and 25% of amplitude on phases a, b and c at t=0.1s (Figure 5(a)). It is worth noting that the technique of filtering and generating the quadrature signal on the α axis does not have a large static error and the reconstructed signal $v'_{\alpha r}$ joins the real signal $v_{\alpha r}$ after a reasonable time as depicted in Figure 5(b). The error between $v'_{\alpha r}$ and $v_{\alpha r}$ is canceled after a short time and the same observation is valid for the β axis. From the perspective of proving the robustness of the sequence separation technique, Figure 6(a) shows the simulation results of the $\alpha\beta$ components of the positive and of the negative sequence. In addition, the positive and negative sequences of the three-phase voltages, which were reconstructed from the detected amplitudes and phase angle are depicted in Figure 6(b).

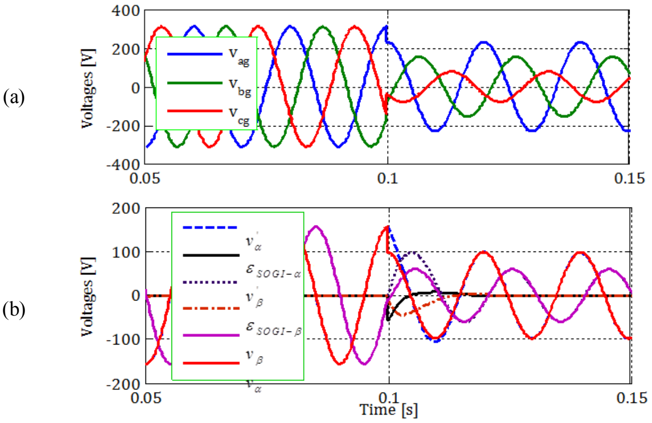

Fig. 5. (a) Unbalanced grid voltages, (b) DSOGI-QSG-based $\alpha\beta$ components generation

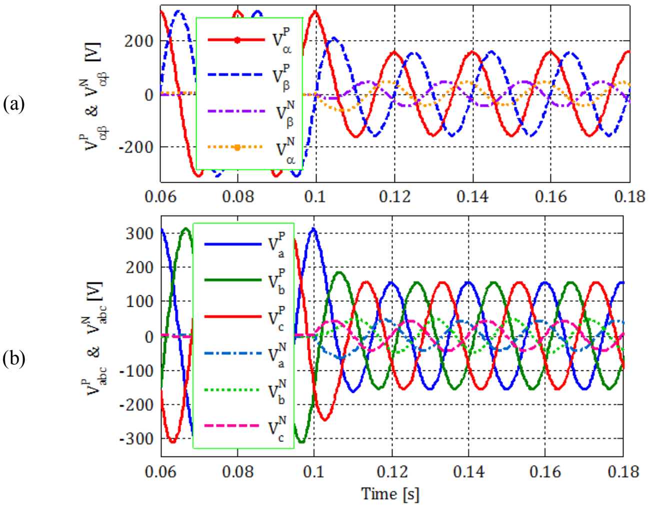

Fig. 6. (a) $\alpha\beta$ components, (b) fundamental component of the three phase postive and negative sequences extracted from grid voltages using SOGI method

The results previously analyzed clearly show the satisfactory performance of the technique used for the separation of symmetrical sequences and the grid synchronization of the command. In the following, special attention is paid to the quality of currents and active and reactive powers exchanged with the utility grid. Indeed, faced with the same fault conditions, the results of simulations of the BPSC approach application show that, although the currents injected into the grid remain sinusoidal balanced and in phase with the corresponding voltages, the amplitude of such currents is increased to maintain the average injected active power when the fault occurs (Figure 7(a)). Unfortunately, we note the presence of oscillations of the second harmonic of the active and reactive powers exchanged with the grid P_g and Q_g. It is important to note that the appearance of these oscillations is expected due to the interaction between the current of the positive sequence and the voltage of the negative sequence in

(16)-(17). This is detrimental to the stability of the power system as shown in Figure 7(b). The examination of Figure 7 and its enlargement of its encircled portions shown in Figure 8 verifies that the currents generated by the SOGI-BA control system are perfectly sinusoidal and balanced even in the presence of the grid fault.

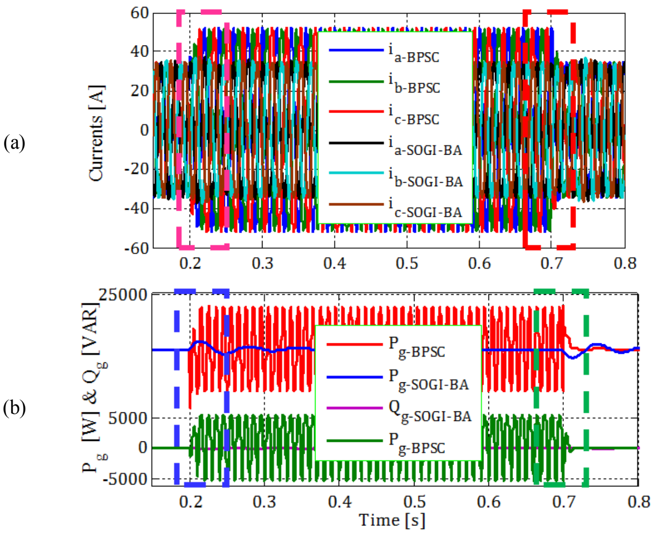

Fig. 7. (a) Grid currents at PCC, (b) exchanged active and reactive powers at PCC

The amplitude of these currents is constant despite the fact that a few minor oscillations are recorded during the appearance and disappearance of the asymmetric three-phase fault (Figure 8(a)). With regard to the active ($P_{SOGI\text{-}BA}$) and reactive ($Q_{SOGI\text{-}BA}$) powers exchanged at the PCC, it is clear that the SOGI-BA approach has succeeded in generating active and reactive powers that are almost insensitive to the occurrence of the asymmetric fault.

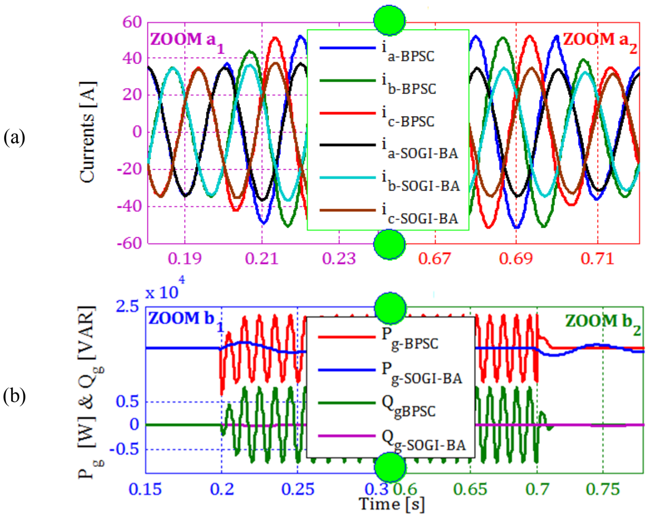

Fig. 8. Zoom version of (a) grid currents at PCC, (b) exchanged active and reactive powers at PCC

Only a few rapidly amortized and canceled fluctuations can be seen at the moments of appearance and disappearance of the studied fault as depicted in Figure 8(b). Figure 8 depicts the expanded portions of Figure 7. Again, we can see that the SOGI-BA control system achieves the best performance regarding power quality standards in terms of delivered currents and exchanged active and reactive power, because it garantees the fictive isolation of the GSC from the fault in the grid.

VI. CONCLUSION

In this paper, a control approach based on second-order generalized integrators (SOGIs) and symmetrical sequences theory was proposed to provide effective support of grid-connected voltage source inverters' operation under non-ideal grid conditions. The proposed control method involves the extraction of the symmetrical sequences of the unbalanced grid voltages using SOGIs, the coordinated control of active and reactive powers and the voltage and current control loops. Simulations developed and programmed in MATLAB environment have proven the performance of the proposed approach in ensuring the service continuity even during asymmetrical grid voltage faults.

ACKNOWLEDGMENT

The author acknowledges the financial support of the Deanship of Scientific Research, University of Hail, Saudi Arabia of this work through the project No. 160978, 2018.

REFERENCES

[1] A. Abbassi, M. A. Dami, M. Jemli, "A statistical approach for hybrid energy storage system sizing based on capacity distributions in an autonomous PV/Wind power generation system", Renewable Energy, Vol. 103, pp. 81-93, 2017

[2] M. A. Destek, A. Aslan, "Renewable and non-renewable energy consumption and economic growth in emerging economies: Evidence from bootstrap panel causality", Renewable Energy, Vol. 111, pp. 757-763, 2017

[3] R. Abbassi, S. Chebbi, "Energy management strategy for a grid-connected wind-solar hybrid system with battery storage: Policy for optimizing conventional energy generation", International Review of Electrical Engineering, Vol. 7, No. 2, pp. 3979-3990, 2012

[4] R. Abbassi, S. Saidi, M. Hammami, S. Chebbi, Analysis of renewable energy power systems: Reliability and flexibility during unbalanced network fault, IGI Global, 2015

[5] R. Abbassi, S. Marrouchi, S. Saidi, A. Abbassi, S. Chebbi, "Optimal energy management strategy and novel control approach for DPGSs under unbalanced grid faults", Journal of Circuits, Systems and Computers, Vol. 28, No. 4, Article ID 1950057, 2019

[6] W. Zhang, A. M. Cantarellas, J. Rocabert, A. Luna, P. Rodriguez, "Synchronous power controller with flexible droop characteristics for renewable power generation systems", IEEE Transactions on Sustainable Energy, Vol. 7, No. 4, pp. 1572–1582, 2016

[7] W. Zhang, D. Remon, A. M. Cantarellas, A. Luna, P. Rodriguez, "Dynamics estimation and generalized tuning of stationary frame current controller for grid tied power converters", European Power Electronics and Drives, Vol. 26, No. 3, pp. 85–95, 2016

[8] R. Abbassi, M. Hammami, S. Chebbi, "Improvement of the integration of a grid-connected wind-photovoltaic hybrid system", International Conference on Electrical Engineering and Software Applications, Hammamet, Tunisia, March 21-23, 2013

[9] R. Abbassi., S. Marrouchi, M. B. Hessine, S. Chebbi, H. Jouini, "Voltage control strategy of an electrical network by the integration of

the UPFC compensator", International Review On Modelling and Simulation, Vol. 5, No. 1, pp. 380–384, 2012

[10] S. Saidi, R. Abbassi, S. Chebbi, "Virtual flux based direct power control of shunt active filter", Scientica Iranica, Transactions on Computer Science & Engineering and Electrical Engineering, Vol. 21, No. 6, pp. 2165-2176, 2014

[11] A. Nouaiti, A. Saad, A. Mesbahi, M. Khafallah, M. Reddak, "Design and test of a new three-phase multilevel inverter for PV system applications", Engineering, Technology & Applied Science Research, Vol. 9, No. 1, pp. 3846-3851, 2019

[12] D. Chen, J. Jiang, Y. Qiu, J. Zhang, F. Huang, "Single-stage three-phase current-source photovoltaic grid-connected inverter high voltage transmission ratio", IEEE Transactions on Power Electronics, Vol. 32, No. 10, pp. 7591-7601, 2017

[13] D. Chen, Y. Qiu, Y. Chen, Y. He, "Nonlinear PWM-controlled single-phase boost mode grid-connected photovoltaic inverter with limited storage inductance current", IEEE Transactions on Power Electronics, Vol. 32, No. 4, pp. 2717-2727, 2017

[14] H. Goh, M. Armstrong, B. Zahawi, "Adaptive control technique for suppression of resonance in grid-connected PV inverters", IET Power Electronics, Vol. 12, No. 6, pp. 1479-1486, 2019

[15] W. Choi, W. Lee, D. Han, B. Sarlioglu, "New configuration of multifunctional grid-connected inverter to improve both current-based and voltage-based power quality", IEEE Transactions on Industry Applications, Vol. 54, No. 6, pp. 6374-6382, 2018

[16] Q. Yan, X. Wu, X. Yuan, Y. Geng, "An improved grid-voltage feedforward strategy for high-power three-phase grid-connected inverters based on the simplified repetitive predictor", IEEE Transactions on Power Electronics, Vol. 31, No. 5, pp. 3880-3897, 2016

[17] X. Zhang, D. Xia, Z. Fu, G. Wang, D. Xu, "An improved feedforward control method considering PLL dynamics to improve weak grid stability of grid-connected inverters", IEEE Transactions on Industry Applications, Vol. 54, No. 5, pp. 5143-5151, 2018

[18] J. Wang, J. D. Yan, L. Jiang, "Pseudo-derivative-feedback current control for three-phase grid-connected inverters with LCL filter", IEEE Transactions on Power Electronics, Vol. 31, No. 5, pp. 3898-3912, 2016

[19] R. Chilipi, N. A. Sayari, K. A. Hosani, A. R. Beig, "Control scheme for grid-tied distributed generation inverter under unbalanced and distorted utility conditions with power quality ancillary services", IET Renewable Power Generation, Vol. 10, No. 2, pp. 140-149, 2016

[20] D. Pan, X. Ruan, C. Bao, W. Li, X. Wang, "Capacitorcurrent feedback active damping with reduced computation delay for improving robustness of LCL-type grid-connected inverter", IEEE Transactions on Power Electronics, Vol. 29, No. 7, pp. 3414–3427, 2014

[21] S. R. K. Hoseini, H. Givi, E. Farjah, T. Ghanbari, "Phase locked loop-free sliding-mode-based power control for grid-connected voltage-sourced inverters under unbalanced network conditions", 8th Power Electronics, Drive Systems & Technologies Conference, Mashhad, Iran, February 14-16, 2017

[22] M. K. Ghartemani, "Linear and pseudolinear enhanced phased-locked loop (EPLL) structures", IEEE Transactions on Industrial Electronics, Vol. 61, No. 3, pp. 1464–1474, 2014

[23] R. Abbassi, A. Boudjemline, A. Abbassi, A. Torchani, H. Gasmi, T. Guesmi, "A numerical-analytical hybrid approach for the identification of SDM solar cell unknown parameters", Engineering Technology & Applied Science Research, Vol. 8, No. 3, pp. 2907-2913, 2018

[24] S. Latreche, A. E. Badoud, M. Khemliche, "Implementation of MPPT algorithm and supervision of shading on photovoltaic module", Engineering, Technology & Applied Science Research, Vol. 8, No. 6, pp. 3541-3544, 2018

[25] P. Rodriguez, A. V. Timbus, R. Teodorescu, M. Liserre, F. Blaabjerg, "Flexible active power control of distributed power generation systems during grid faults", IEEE Transactions on Industrial Electronics, Vol. 54, No. 5, pp. 2583-2592, 2007